High-pressure Synthesis and Crystal Structure of the Borate $Sc_3B_5O_{12}$

Stephanie C. Neumair and Hubert Huppertz

Institut für Allgemeine, Anorganische und Theoretische Chemie, Leopold-Franzens-Universität Innsbruck, Innrain 52a, 6020 Innsbruck, Austria

Reprint requests to H. Huppertz. E-mail: Hubert.Huppertz@uibk.ac.at

Z. Naturforsch. **2009**, *64b,* 1339 – 1344; received September 27, 2009

Dedicated to Professor Hubert Schmidbaur on the occasion of his 75th birthday

The rare-earth borate $Sc_3B_5O_{12}$ was synthesized under high-pressure / high-temperature conditions of 6 GPa and 1100 °C in a Walker-type multianvil apparatus. The single-crystal structure determination revealed an isotypy to $RE_3B_5O_{12}$ (*RE* = Er–Lu). $Sc_3B_5O_{12}$ crystallizes in the rare space group *Pmna* ($Z = 4$) with the parameters $a = 1245.4(3)$, $b = 443.46(9)$, $c = 1222.1(2)$ pm, $V = 0.675(1)$ nm^3, $R_1 = 0.0520$, and $wR_2 = 0.0860$ (all data). The structure of $Sc_3B_5O_{12}$ is composed of layers of condensed BO_4 tetrahedra, separated by eight-fold coordinated scandium ions.

Key words: Borate, Crystal Structure

Introduction

Over the last decade, high-pressure / high-temperature studies in the field of rare-earth borates led to a huge variety of new polymorphs and compositions. We were able to synthesize several new polymorphs of known compositions, *e. g.* β-/γ-/δ-$RE(BO_2)_3$ [1 – 4], χ-REBO$_3$ (*RE* = Dy, Er) [5], and ν-DyBO$_3$ [6]. New compositions like $Pr_4B_{10}O_{21}$ [7], α-$RE_2B_4O_9$ (*RE* = Sm–Tb, Ho [8 – 11]), β-$RE_2B_4O_9$ (*RE* = Dy, Gd [12, 13]), $RE_4B_6O_{15}$ (*RE* = Dy, Ho [11, 14, 15]), and $RE_3B_5O_{12}$ (*RE* = Er–Lu [16]) extended the structural chemistry of oxoborates. As a common trend, with increasing pressure boron atoms favor the four-fold coordination, as expected from the pressure-coordination rule [17]. Additionally, it was observed that these BO_4 tetrahedra, normally linked *via* common corners, can form even denser structures by sharing common edges. Examples are the phases α-$RE_2B_4O_9$ (*RE* = Sm–Tb, Ho) [8 – 11] and $RE_4B_6O_{15}$ (*RE* = Dy, Ho) [11, 14, 15], in which 1/10th and 1/3rd of the tetrahedra possess a common edge to a second BO_4 tetrahedron, respectively. This connection could also be realized in the recently synthesized compounds HP-NiB_2O_4 [18] and β-FeB_2O_4 [19], which are the first borates exhibiting exclusively BO_4 tetrahedra with a common edge to another one. Furthermore, in several borates, there could be found partially increased coordination spheres of the oxygen ($O^{[2]} \rightarrow O^{[3]}$) and rare-earth atoms.

Recently, we turned to scandium borates under extreme conditions. To the best of our knowledge, the ternary system Sc-B-O exhibits only the compound $ScBO_3$ [20]. This borate crystallizes in a trigonal calcite structure, consisting of alternating layers of scandium atoms and trigonal-planar BO_3 units. Systematic investigations into the ternary system Sc-B-O under high-pressure / high-temperature conditions led to the here presented new high-pressure borate $Sc_3B_5O_{12}$, which is isotypic to the above mentioned phases $RE_3B_5O_{12}$ (*RE* = Er–Lu [16]). We describe the synthesis, the crystal structure, and the properties of $Sc_3B_5O_{12}$, as well as the similarities and differences to the isotypic rare-earth borates $RE_3B_5O_{12}$ (*RE* = Er–Lu [16]) and to the homeotype mineral semenovite.

Experimental Section

Synthesis

The compound $Sc_3B_5O_{12}$ was synthesized under high-pressure / high-temperature conditions of 6 GPa and 1100 °C. For the synthesis of $Sc_3B_5O_{12}$, a stoichiometric mixture of Sc_2O_3 (Sigma-Aldrich Chemie GmbH, Munich, Germany, 99.9 %) and B_2O_3 (Strem Chemicals, Newburyport, USA, 99.9 %) was ground up and filled into a boron nitride crucible (Henze BNP GmbH, HeBoSint® S10, Kempten, Germany). The crucible was placed into an 18/11 assembly, which was compressed by eight tungsten carbide cubes (TSM-20, Ceratizit, Reutte, Austria). The pressure was applied *via* a Walker-type multianvil device and a 1000 t press (both devices from

the company Voggenreiter, Mainleus, Germany). A detailed description of the assembly and its preparation can be found in refs. [21 – 25]. The assembly was compressed to 6 GPa within 2.5 h and kept at this pressure for the heating period. The sample was heated to 1100 °C in 10 min, kept there for 20 min, and cooled down to 450 °C in 20 min. Afterwards, the sample was naturally cooled down to r. t. by switching off the heating, followed by a decompression period of 7.5 h. The recovered pressure medium was broken apart and the surrounding boron nitride crucible removed from the sample. The compound $Sc_3B_5O_{12}$ is an air- and water-resistant, colorless crystalline solid. Up to now, $Sc_3B_5O_{12}$ could not be synthesized as a phase-pure sample. Side products were the unreacted remains of the starting materials Sc_2O_3 and B_2O_3, as well as impurities from the crucible material (hex. BN).

Crystal structure analysis

The powder diffraction pattern of $Sc_3B_5O_{12}$ was obtained in transmission geometry from a flat sample of the reaction product, using a STOE STADI P powder diffractometer with monochromatized MoK_α (λ = 71.073 pm) radiation. The corresponding reflections of the diffraction pattern were indexed and refined on the basis of an orthorhombic unit cell with the program TREOR [26 –28]. The lattice parameters (Table 1) were calculated from least-squares fits of the powder data. The correct indexing of the pattern of $Sc_3B_5O_{12}$ was confirmed by intensity calculations, taking the atomic positions from the structure refinement [29]. The lattice parameters determined from the powder data and the single-crystal data fit well.

For the single-crystal structure analysis, small irregularly shaped crystals of $Sc_3B_5O_{12}$ were isolated by mechanical fragmentation. Measurements of the single-crystal intensity data took place at room temperature by a Nonius Kappa CCD 4-circle diffractometer, equipped with graphite-monochromatized MoK_α (λ = 71.073 pm) radiation, a Micracol Fiber Optics collimator, and a Nonius FR590 generator. For the intensity data of $Sc_3B_5O_{12}$, a numerical absorption correction was applied to the intensity data of $Sc_3B_5O_{12}$ with the program X-SHAPE [30, 31]. The positional parameters of the isotypic compound $Lu_3B_5O_{12}$ were used as starting values for the structural refinement of $Sc_3B_5O_{12}$ (SHELXL-97 [32]). All atoms were refined with anisotropic displacement parameters. The final difference Fourier syntheses did not reveal any significant peaks in the refinements. All relevant details of the data collections and evaluations are listed in Table 1. The Tables 2 – 5 show the positional parameters, the interatomic distances, and angles.

Further details of the crystal structure investigation may be obtained from the Fachinformationszentrum Karlsruhe, D-76344 Eggenstein-Leopoldshafen, Germany (fax: +49-7247-808-666; e-mail: crysdata@fiz-karlsruhe.de, http://

Table 1. Crystal data and structure refinement of $Sc_3B_5O_{12}$ (standard deviations in parentheses).

Empirical formula	$Sc_3B_5O_{12}$
Molar mass, g mol^{-1}	380.93
Crystal system	orthorhombic
Space group	*Pmna*
Powder diffractometer	STOE Stadi P
Radiation	MoK_α (λ = 71.073 pm)
Powder data	
a, pm	1247.8(6)
b, pm	444.2(2)
c, pm	1223.8(5)
Single-crystal diffractometer	Nonius Kappa CCD
Radiation	MoK_α (λ = 71.073 pm) (graphite monochromator)
Single-crystal data	
a, pm	1245.4(3)
b, pm	443.46(9)
c, pm	1222.1(2)
V, nm^3	0.6750(2)
Formula units per cell	Z = 4
Calculated density, g cm^{-3}	3.75
Crystal size, mm^3	0.03 × 0.03 × 0.05
Temperature, K	293(2)
Detector distance, mm	36
Exposure time, min	3
Absorption coefficient, mm^{-1}	3.0
F(000), e	736
θ range, deg	2.3 – 32.5
Range in *hkl*	±18, ±6, ±18
Total no. of reflections	18436
Independent reflections / R_{int}	1279 / 0.1143
Reflections with $I \geq 2\,\sigma(I)$ / R_σ	1054 / 0.0395
Data / ref. parameters	1279 / 101
Absorption correction	numerical [30, 31]
Goodness-of-fit on F^2	1.098
Final indices $R1$ / $wR2$ [$I \geq 2\sigma(I)$]	0.0376 / 0.0821
Indices $R1$ / $wR2$ (all data)	0.0520 / 0.0860
Largest diff. peak / hole, e Å^{-3}	0.73 / −0.57

Table 2. Atomic coordinates and isotropic equivalent displacement parameters U_{eq} (Å^2) of $Sc_3B_5O_{12}$ (space group: *Pmna*) (standard deviations in parentheses). U_{eq} is defined as one third of the trace of the orthogonalized U_{ij} tensor.

Atom	W.-position	*x*	*y*	*z*	U_{eq}
Sc1	4*e*	0.13017(5)	0	1/2	0.0038(2)
Sc2	8*i*	0.36430(3)	0.9880(2)	0.69523(3)	0.0041(2)
B1	4*f*	0.3380(3)	1/2	1/2	0.0036(6)
B2	8*i*	0.2975(2)	0.4576(6)	0.8501(2)	0.0040(5)
B3	4*h*	0	0.4658(9)	0.3549(3)	0.0044(6)
B4	4*h*	0	0.5409(9)	0.8694(3)	0.0041(6)
O1	4*h*	0	0.2376(5)	0.4362(2)	0.0040(4)
O2	4*h*	0	0.2250(6)	0.8550(2)	0.0045(4)
O3	8*i*	0.2963(2)	0.7802(4)	0.8468(2)	0.0041(3)
O4	8*i*	0.4053(2)	0.3269(4)	0.8579(2)	0.0041(3)
O5	8*i*	0.4032(2)	0.3331(4)	0.4217(2)	0.0035(3)
O6	4*g*	1/4	0.3207(6)	3/4	0.0037(4)
O7	4*h*	1/2	0.7024(5)	0.7425(2)	0.0038(4)
O8	8*i*	0.2666(2)	0.2955(4)	0.5626(2)	0.0045(3)

Table 3. Interatomic B–O distances (pm) in $Sc_3B_5O_{12}$ (space group: *Pmna*), calculated with the single-crystal lattice parameters (standard deviations in parentheses).

B1–O5a	145.7(2)	B2–O3	143.1(3)	B3–O1	141.9(4)	B4–O2	141.2(4)
B1–O5b	145.7(2)	B2–O4	146.5(3)	B3–O4a	149.6(3)	B4–O5a	147.4(3)
B1–O8a	148.3(3)	B2–O6	148.9(3)	B3–O4b	149.6(3)	B4–O5c	147.4(3)
B1–O8b	148.3(3)	B2–O8	151.4(3)	B3–O7	156.3(4)	B4–O7	154.3(4)
	av. = 147.0		av. = 147.5		av. = 149.4		av. = 147.6
			— av. over all B–O distances: 147.9 —				

Table 4. Interatomic angles (deg) of $Sc_3B_5O_{12}$ (space group: *Pmna*), based on single-crystal data (standard deviations in parentheses).

O5a–B1–O5b	112.3(3)	O3–B2–O4a	114.1(2)	O1–B3–O4a	114.9(2)	O2–B4–O5a	115.5(2)
O5a–B1–O8a	107.8(2)	O3–B2–O6	112.3(2)	O1–B3–O4b	114.9(2)	O2–B4–O5c	115.5(2)
O5a–B1–O8b	111.26(9)	O4a–B2–O6	104.8(2)	O4a–B3–O4b	104.1(3)	O5a–B4–O5c	109.7(3)
O5b–B1–O8b	111.26(9)	O3–B2–O8a	119.3(2)	O1–B3–O7a	106.0(3)	O2–B4–O7b	110.5(3)
O5b–B1–O8a	107.8(2)	O4a–B2–O8a	104.5(2)	O4a–B3–O7a	108.3(2)	O5a–B4–O7b	102.0(2)
O8a–B1–O8b	106.3(2)	O6–B2–O8a	100.1(2)	O4b–B3–O7a	108.3(2)	O5c–B4–O7b	102.0(2)
	av. = 109.5		av. = 109.2		av. = 109.4		av. = 109.2

Table 5. Interatomic Sc–O distances (pm) in $Sc_3B_5O_{12}$ (space group: *Pmna*), calculated with the single-crystal lattice parameters (standard deviations in parentheses).

Sc1–O1a	208.5(2)	Sc2–O2	208.3(2)
Sc1–O1b	208.5(2)	Sc2–O5	207.4(2)
Sc1–O3a	230.2(2)	Sc2–O6	215.6(2)
Sc1–O3b	230.2(2)	Sc2–O7	218.9(2)
Sc1–O8a	227.8(2)	Sc2–O3a	223.5(2)
Sc1–O8b	227.8(2)	Sc2–O3b	226.1(2)
Sc1–O4a	230.5(2)	Sc2–O8	244.3(2)
Sc1–O4b	230.5(2)	Sc2–O4	254.4(2)
	av. = 224.3		av. = 224.8
	— av. over all Sc–O distances: 224.6 —		

www.fiz-informationsdienste.de/en/DB/icsd/depot_anforderung.html) on quoting the deposition number CSD-421030.

Results and Discussion

The crystal structure of $Sc_3B_5O_{12}$ is isotypic to the structures of $RE_3B_5O_{12}$ (RE = Er–Lu) [16]. In analogy, the latter compounds were also synthesized under high-pressure / high-temperature conditions, but at higher pressures of 10 GPa and temperatures of 1100 °C. Fig. 1 shows the crystal structure of $Sc_3B_5O_{12}$, based on layers of distorted corner-sharing BO_4 tetrahedra, which are separated by Sc^{3+} ions. Like in most high-pressure phases of the borates, we only observe BO_4 tetrahedra, as for example in α-$RE_2B_4O_9$ (RE = Sm–Tb, Ho [8 – 11]), $RE_4B_6O_{15}$ (RE = Dy, Ho [11, 14, 15]), β-MB_4O_7 (M = Mn [33], Co [34], Fe [34], Ni [33], Cu [33], Zn [35]), and the phases HP-NiB_2O_4 [18] and β-FeB_2O_4 [19].

Only one tetrahedron (B(1), Q^4, light polyhedra) shares all four vertices with other tetrahedra, while

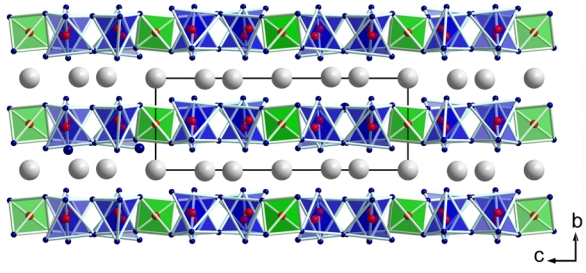

Fig. 1. Crystal structure of $Sc_3B_5O_{12}$ with a view along [$\bar{1}$00]. Light (green) shaded polyhedra represent Q^4-bonded BO_4 tetrahedra, dark polyhedra (blue) show Q^3 tetrahedra (color online).

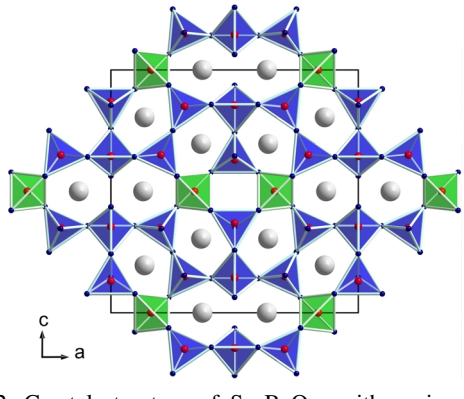

Fig. 2. Crystal structure of $Sc_3B_5O_{12}$ with a view along [010]. Light (green) polyhedra and dark polyhedral (blue) represent Q^4- and Q^3-bonded BO_4 tetrahedra, respectively (color online).

the remaining ones (B(2)–B(4), Q^3, dark polyhedra) show one unshared oxygen atom. As depicted in Fig. 2, eight-, five-, and four-membered rings are formed

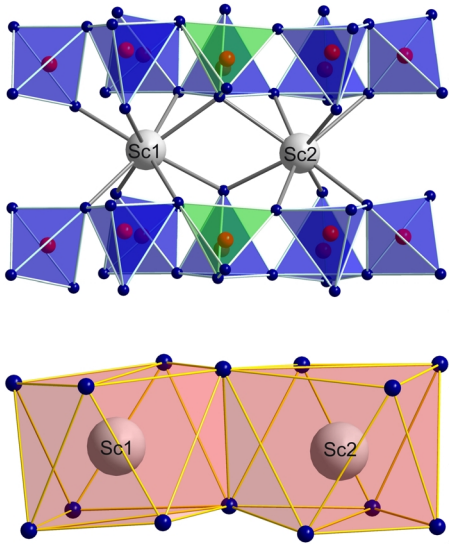

Fig. 3. Coordination spheres of Sc^{3+} (grey spheres) in the crystal structure of $Sc_3B_5O_{12}$ (color online).

from the BO_4 tetrahedra inside the layers. All rings lie in the *ac* plane at a height of $1/2$ *b*. The eight-membered rings are formed by two Q^4 and six Q^3 tetrahedra. These rings are interconnected along the *a* axis by two tetrahedra, forming four-membered rings, which are situated on the edges and in the center of the unit cell. Inside the four-membered ring, Q^4 (B1) and Q^3 (B2) tetrahedra occur in alternate positions. Two adjacent tetrahedra of the four-membered ring shape a five-membered ring with three additional BO_4 tetrahedra, belonging to two different eight-membered rings. Fig. 1 shows that the scandium ions are positioned between the five- and eight-membered rings.

In $Sc_3B_5O_{12}$, the B–O distances vary between 141.2 and 156.3 pm and average out to 147.9 pm (Table 3). This value is in good agreement with the known average value of 147.0 pm [36, 37] for the B–O bond length in BO_4 tetrahedra. In comparison, the average B–O bond lengths in $RE_3B_5O_{12}$ (*RE* = Er–Lu) [16] are slightly larger with the average values of 149.4 pm (*RE* = Er, Tm), 148.9 pm (*RE* = Yb), and 149.2 pm (*RE* = Lu). As shown in Table 4, the B–O–B angles in the BO_4 tetrahedra in $Sc_3B_5O_{12}$ vary between 100.1 and 119.3°. The isotypic compounds $RE_3B_5O_{12}$ (*RE* = Er–Lu) also show distorted BO_4 tetrahedra with B–O–B angles of 99.8 – 117.3° for $Er_3B_5O_{12}$, 98.2 – 118.2° for $Tm_3B_5O_{12}$, 99.6 – 117.3° for $Yb_3B_5O_{12}$, and 99.1 – 118.8° for $Lu_3B_5O_{12}$.

Table 6. Comparison of the lattice parameters (pm), volumes (nm^3), and ionic radii (pm) of $RE_3B_5O_{12}$ (*RE* = Sc, Er–Lu).

Compound	*a*	*b*	*c*	*V*	$r(RE^{3+})$ [47, 48]
$Sc_3B_5O_{12}$	1245.4(3)	443.46(9)	1222.1(2)	0.6750(2)	101.0
$Er_3B_5O_{12}$	1286.1(5)	462.2(2)	1253.1(4)	0.7449(6)	111.7
$Tm_3B_5O_{12}$	1280.5(4)	460.2(2)	1248.1(4)	0.7355(5)	112.5
$Yb_3B_5O_{12}$	1277.8(2)	458.96(4)	1245.1(2)	0.7302(2)	113.4
$Lu_3B_5O_{12}$	1274.7(5)	457.1(2)	1242.4(5)	0.7240(7)	114.4

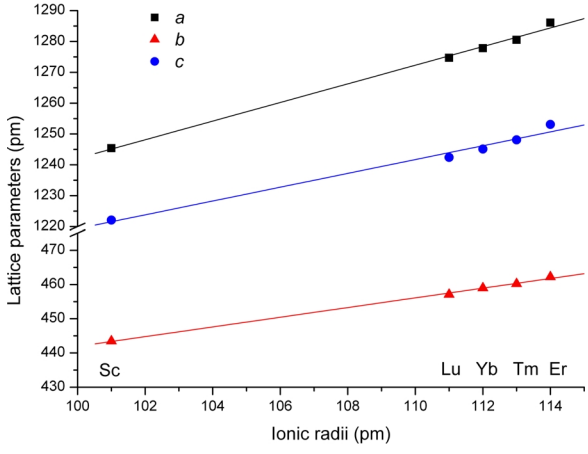

Fig. 4. Illustration of the coherence of the ionic radii and the lattice parameters *a*, *b*, and *c* in $RE_3B_5O_{12}$ (*RE* = Sc, Er–Lu).

The two crystallographically independent Sc^{3+} ions are coordinated by eight oxygen atoms each, forming two distorted square antiprisms (Fig. 3). The Sc^{3+} distances vary from 207.4 to 254.4 pm with a mean value of 224.6 pm (Table 5). Similar Sc–O distances for eight-fold coordinated Sc^{3+} were found in the high-pressure phase $ScAlO_3$ (206.9 – 255.4 pm, av. = 227.3 pm) [38].

The bond valence sums for all atoms of $Sc_3B_5O_{12}$ were calculated, using the bond length / bond strength (ΣV) [39, 40] and the CHARDI concept (*char*ge *di*stribution in solids, ΣQ) [41]. The results of both concepts confirm the supposed formal ionic charges, resulting from the crystal structure [ΣV: +2.85 (Sc1), +2.94 (Sc2), +3.06 (B1), +3.04 (B2), +2.90 (B3), +3.04 (B4), −1.94 (O1), −1.97 (O2), −1.82 (O3), −1.78 (O4), −2.08 (O5), −2.32 (O6), −2.01 (O7), − 1.73 (O8), and ΣQ: +3.06 (Sc1), +2.95 (Sc2), +3.03 (B1), +3.03 (B2), +3.05 (B3), +2.90 (B4), −2.10 (O1), −2.09 (O2), −1.91 (O3), −1.91 (O4), −2.11 (O5), −2.34 (O6), −1.91 (O7), −1.85 (O8)].

The MAPLE values (*ma*delung *p*art of *l*attice *e*nergy) [42 – 44] were calculated in order to com-

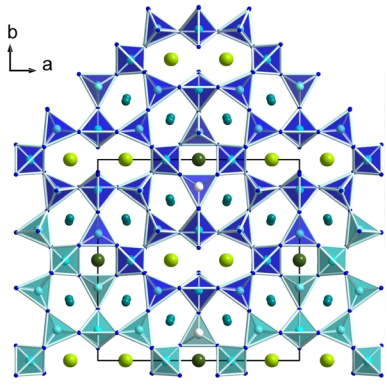

Fig. 5. Crystal structure of the mineral *semenovite* [$(Fe^{2+}$, Mn, Zn, Ti)RE_2Na_{0-2}(Ca, Na)$_8$(Si, Be)$_{20}$(O, OH, F)$_{48}$, space group: *Pmnn*] [49, 50]; view along [00$\bar{1}$]. Polyhedra: (Si/Be)O_4 tetrahedra; white spheres: fluoride; large light (green) spheres: rare-earth, sodium; large dark (green) spheres: iron, manganese, zinc, titanium; small dark spheres: calcium, sodium. The dark shaded polyhedra visualize the identity of the topology of the tetrahedral layers in *semenovite* and $RE_3B_5O_{12}$ (*RE* = Sc, Er–Lu) (Fig. 1) (color online).

pare the results with the MAPLE values received from Sc_2O_3 [45] and the high-pressure modification B_2O_3-II [46]. This can be managed by the additive potential of the MAPLE values, which allows to calculate hypothetical values for $Sc_3B_5O_{12}$, starting from the binary oxides. As a result, we obtained a value of 79279 kJ mol^{-1} for $Sc_3B_5O_{12}$ to be compared with 79546 kJ mol^{-1} (deviation 0.3 %), starting from the binary oxides (1.5 × Sc_2O_3 (16467 kJ mol^{-1}) [45] + 2.5 × B_2O_3-II (21938 kJ mol^{-1}) [46]).

A comparison of the lattice parameters, cell volumes, and rare-earth metal ionic radii [47, 48] of $RE_3B_5O_{12}$ (*RE* = Sc, Er–Lu) is given in Table 6, while Fig. 4 illustrates the coherence of the ionic radii and the lattice parameters *a*, *b*, and *c* in $RE_3B_5O_{12}$ (*RE* = Sc, Er–Lu). As expected, the decrease of the lattice parameters corresponds to the decrease of the ionic radii of the rare-earth cations.

As depicted in Fig. 5, the borates $RE_3B_5O_{12}$ (*RE* = Sc, Er–Lu) have an interesting homeotype structure, known from the beryllo-silicate mineral *semenovite* [$(Fe^{2+}$, Mn, Zn, Ti)RE_2Na_{0-2}(Ca, Na)$_8$(Si, Be)$_{20}$(O, OH, F)$_{48}$] [49, 50], consisting of topologically identical condensed layers of BeO_4 and SiO_4 tetrahedra. *Semenovite* has an enlarged unit cell, which is essential for ordering the metal atoms and the tetrahedral centers with Be/Si. In $RE_3B_5O_{12}$ (*RE* = Sc, Er–Lu), the first rare-earth site *RE*(1) lies in between the centers of the five-membered rings, while the cavities between the eight-membered rings are completely filled with *RE*(2). In *semenovite*, metal ions hold these positions. Additionally, the positions between the centers of the four-membered rings are partially occupied, while in $RE_3B_5O_{12}$ (*RE* = Sc, Er–Lu) this site is empty. Due to this site, the consequence of a group-subgroup relationship between the rare-earth borate and *semenovite* is inadmissible. Nevertheless, the here presented rare-earth oxoborate exhibits a homeotype structure to the beryllo-silicate *semenovite*.

Conclusions

This paper presents the high-pressure / high-temperature synthesis and structural characterization (single-crystal data) of the second known ternary scandium borate $Sc_3B_5O_{12}$. It is isotypic to the oxoborates $RE_3B_5O_{12}$ (*RE* = Er–Lu) [16] and consists of layers of corner-sharing BO_4 tetrahedra, that are separated and charge-balanced by Sc^{3+} ions. The structure type is homeotype to the beryllo-silicate *semenovite*.

Acknowledgements

We would like to thank Dr. G. Heymann for collecting the single-crystal data. This work was financially supported by the Deutsche Forschungsgemeinschaft (HU 966/2-3) and the Fonds der Chemischen Industrie.

[1] H. Emme, T. Nikelski, Th. Schleid, R. Pöttgen, M. H. Möller, H. Huppertz, *Z. Naturforsch.* **2004**, *59b*, 202.
[2] H. Emme, C. Despotopoulou, H. Huppertz, *Z. Anorg. Allg. Chem.* **2004**, *630*, 2450.
[3] G. Heymann, T. Soltner, H. Huppertz, *Solid State Sci.* **2006**, *8*, 821.
[4] A. Haberer, G. Heymann, H. Huppertz, *Z. Naturforsch.* **2007**, *62b*, 759.
[5] H. Huppertz, B. von der Eltz, R.-D. Hoffmann, H. Piotrowski, *J. Solid State Chem.* **2002**, *166*, 203.
[6] H. Emme, H. Huppertz, *Acta Crystallogr.* **2005**, *C61*, i117.
[7] A. Haberer, G. Heymann, H. Huppertz, *J. Solid State Chem.* **2007**, *180*, 1595.
[8] H. Emme, H. Huppertz, *Z. Anorg. Allg. Chem.* **2002**, *628*, 2165.
[9] H. Emme, H. Huppertz, *Chem. Eur. J.* **2003**, *9*, 3623.
[10] H. Emme, H. Huppertz, *Acta Crystallogr.* **2005**, *C61*, i29.

[11] H. Huppertz, H. Emme, *J. Phys.: Condens. Matter* **2004**, *16*, 1283.
[12] H. Huppertz, S. Altmannshofer, G. Heymann, *J. Solid State Chem.* **2003**, *170*, 320.
[13] H. Emme, H. Huppertz, *Acta Crystallogr.* **2005**, *C61*, i23.
[14] H. Huppertz, B. von der Eltz, *J. Am. Chem. Soc.* **2002**, *124*, 9376.
[15] H. Huppertz, *Z. Naturforsch.* **2003**, *58b*, 278.
[16] H. Emme, M. Valldor, R. Pöttgen, H. Huppertz, *Chem. Mater.* **2005**, *17*, 2707.
[17] A. Neuhaus, *Chimia* **1964**, *18*, 93.
[18] J. S. Knyrim, F. Roeßner, S. Jakob, D. Johrendt, I. Kinski, R. Glaum, H. Huppertz, *Angew. Chem.* **2007**, *119*, 9256; *Angew. Chem. Int. Ed.* **2007**, *46*, 9097.
[19] S. Neumair, R. Glaum, H. Huppertz, *Z. Naturforsch.* **2009**, *64b*, 883.
[20] D. A. Keszler, H. Sun, *Acta Crystallogr.* **1988**, *C44*, 1505.
[21] N. Kawai, S. Endo, *Rev. Sci. Instrum.* **1970**, *41*, 1178.
[22] D. Walker, M. A. Carpenter, C. M. Hitch, *Am. Mineral.* **1990**, *75*, 1020.
[23] D. Walker, *Am. Mineral.* **1991**, *76*, 1092.
[24] D. C. Rubie, *Phase Transitions* **1999**, *68*, 431.
[25] H. Huppertz, *Z. Kristallogr.* **2004**, *219*, 330.
[26] P.-E. Werner, TREOR90, University of Stockholm, **1990**.
[27] P.-E. Werner, *Z. Kristallogr.* **1964**, *120*, 375.
[28] P.-E. Werner, L. Errikson, M. Westdahl, *J. Appl. Crystallogr.* **1985**, *18*, 367.
[29] STOE WINXPOW (version 1.2), STOE & Cie GmbH, Darmstadt (Germany) **2001**.
[30] STOE X-SHAPE (version 1.05), STOE & Cie GmbH, Darmstadt (Germany) **1999**.
[31] W. Herrendorf, H. Bärnighausen, HABITUS, *Program for Numerical Absorption Correction*, Universities of Karlsruhe and Giessen, Karlsruhe, Giessen (Germany) **1993/1997**.
[32] G. M. Sheldrick, SHELXS/L-97, Programs for Crystal Structure Determination, University of Göttingen, Göttingen (Germany) **1997**. See also: G. M. Sheldrick, *Acta Crystallogr.* **2008**, *A64*, 112.
[33] J. S. Knyrim, J. Friedrichs, S. Neumair, F. Roeßner, Y. Floredo, S. Jakob, D. Johrendt, R. Glaum, H. Huppertz, *Solid State Sci.* **2008**, *10*, 168.
[34] S. C. Neumair, J. S. Knyrim, R. Glaum, H. Huppertz, *Z. Anorg. Allg. Chem.* **2009**, *635*, 2002.
[35] H. Huppertz, G. Heymann, *Solid State Sci.* **2003**, *5*, 281.
[36] F. C. Hawthorne, P. C. Burns, J. D. Grice, in *Boron: Mineralogy, Petrology and Geochemistry*, (Ed.: E. S. Grew), Mineralogical Society of America, Washington, **1996**.
[37] E. Zobetz, *Z. Kristallogr.* **1990**, *191*, 45.
[38] W. Sinclair, R. A. Eggleton, A. E. Ringwood, *Z. Kristallogr.* **1979**, *149*, 307.
[39] I. D. Brown, D. Altermatt, *Acta Crystallogr.* **1985**, *B41*, 244.
[40] N. E. Brese, M. O'Keeffe, *Acta Crystallogr.* **1991**, *B47*, 192.
[41] R. Hoppe, S. Voigt, H. Glaum, J. Kissel, H. P. Müller, K. J. Bernet, *J. Less-Common Met.* **1989**, *156*, 105.
[42] R. Hoppe, *Angew. Chem.* **1966**, *78*, 52; *Angew. Chem., Int. Ed. Engl.* **1966**, *5*, 95.
[43] R. Hoppe, *Angew. Chem.* **1970**, *82*, 7; *Angew. Chem., Int. Ed. Engl.* **1970**, *9*, 25.
[44] R. Hübenthal, M. Serafin, R. Hoppe, MAPLE (version 4.0), Program for the Calculation of Distances, Angles, Effective Coordination Numbers, Coordination Spheres, and Lattice Energies, University of Gießen, Gießen (Germany) **1993**.
[45] A. Bartos, K. P. Lieb, M. Uhrmacher, D. Wiarda, *Acta Crystallogr.* **1993**, *B49*, 165.
[46] C. T. Prewitt, R. D. Shannon, *Acta Crystallogr.* **1968**, *B24*, 869.
[47] R. D. Shannon, C. T. Prewitt, *Acta Crystallogr.* **1969**, *B25*, 925.
[48] R. D. Shannon, *Acta Crystallogr.* **1976**, *A32*, 751.
[49] O. V. Petersen, J. G. Rönsbo, *Lithos* **1972**, *5*, 163.
[50] F. Mazzi, L. Ungaretti, A. Dal Negro, O. V. Petersen, J. G. Rönsbo, *Am. Mineral.* **1979**, *64*, 202.